Copper nanostructures modified laser scribed electrodes based on graphitic carbon for electrochemical detection of dopamine and glucose

Vuslat B. Juska* and Gediminas Juska

Tyndall National Institute, University College Cork, Ireland

Vuslat.Juska@tyndall.ie

Abstract

BACKGROUND: Carbon-based nanostructures have been attracting major interest in many research fields, including chemical and biological sensing, due to their unique structural dimensions and excellent physical, chemical and mechanical properties. A recently developed laser scribing approach allows design and fabrication of flexible, graphitic carbon based substrates for (bio)-electrochemical applications, as it provides highly robust and low-cost sensing platforms. RESULTS: Here we demonstrate fabrication of a highly reproducible laser scribed graphitic electrodes (LSE) on a polyimide (Kapton) film by using a simple, do-it-yourself laser engraving system equipped with a 405 nm wavelength laser. Copper nanostructures were deposited onto an electrode surface *via* the electrodeposition process. The developed three dimensional graphitic electrodes modified by nano copper/copper oxide species (LSE-Cu) were used for the detection of dopamine and glucose. Electrochemical studies of LSE-Cu showed that in the presence of nano-copper there is an apparent shift of the oxidation peaks of dopamine and ascorbic acid allowing determination of dopamine without an interference effect with an excellent sensitivity of 1321.54 $\mu A\ mM^{-1}\ cm^{-2}$. Furthermore, LSE-Cu sensor exhibited highly satisfying analytical performance toward glucose electro-oxidation with the reproducibility of 5.47 % (RSD %). CONCLUSION: We have demonstrated a simple design, fabrication and passivation route for the preparation of the LSEs performing as biosensors. Such cost-effective and design-flexible system is highly suitable to develop biosensing platform towards various target analytes and further miniaturization of the electrode.

Key words

Laser scribed electrode, graphitic carbon, graphene, dopamine detection, glucose detection

Introduction

Numerous carbon materials have been studied extensively in the construction of biosensors as either nanostructures for matrix development or standalone electrodes(1). Considering the rich reputation of

This article has been accepted for publication and undergone full peer review but has not been through the copyediting, typesetting, pagination and proofreading process which may lead to differences between this version and the Version of Record. Please cite this article as doi: 10.1002/jctb.6620

carbon based materials in electrochemical application, it is hardly surprising that graphene, in particular, has become a hot topic of electrochemical sciences over the recent years. Its water-dispersible derivatives, such as graphene oxide, are often used for surface chemistry processes of electrodes. However, even when reduced through physico/chemical steps, the excellent electrical properties of pristine graphene cannot be obtained due to multiple defects in graphene oxide(2, 3). A breakthrough has been achieved in 2012, when an attractive, technologically simple and cheap approach has been reported by El-Kady *et al*.(4) who described a strategy for the production of reduced graphene oxide based electrochemical capacitors. In that work, graphene oxide (GO) dispersion in water was drop-casted on a flexible substrate and, in order to reduce to graphene, irradiated by an infrared laser integrated in a commercially available LightScribe CD/DVD optical drive. This research opened up a new era in the field of electrochemical biosensors, in particular, flexible sensors due to an easy and cost-effective preparation of graphene and graphite based electrodes by a simple laser irradiation. For instance, in 2014 Griffiths *et al.*(5) used the same technology to produce laser scribed electrodes for electrochemical sensor applications. In the same year, a broad study of commercially available polyimide sheet (Kapton) conversion into graphitic carbon by a direct-write laser scribing process has been shown publicly for the first time(6). In 2016 Nayak *et al.*(7) reported the fabrication of flexible electrochemical sensors using the latter fabrication method. The scribed structures have self-standing porous 3D morphology and abundant edge planes which are of a great advantage to apply several surface chemistry applications for the development of biosensors. In 2017 Fenzl *et al.*(3) have demonstrated the use of such electrodes as biomolecules' immobilization platform for aptamer based detection technologies. They simply attached the aptamers to the surface of laser-scribed graphene electrodes via π-stacking and hydrophobic interactions between the graphene and the pyrene of the anchoring molecule. The developed biosensor displayed extremely low detection limits towards the analyte in a complex matrix of serum. In 2018 Lin *et al.*(8) have reported the use of copper nanoparticles electrodeposited, DVD-laser scribed graphene electrodes for glucose oxidation. In the same year, Xu *et al.*(9) have demonstrated a laser scribed graphene electrode which was modified with PEDOT to be used for dopamine detection. Another initiative approach has been reported by Chyan *et al.*(10) in 2018. In this study researchers have implemented a laser writing process of graphene patterning on surfaces of various materials with high lignin content, such as food, cloth, paper, cardboard, high-performance polymers and natural coal, essentially demonstrating vast potential in niche applications – cheap, flexible, biodegradable and edible electronics.

The research field of electrochemical glucose biosensors has shown an outstanding growth and development since the first enzyme electrode towards glucose discovered in 1962 by Clark and Lyons(11). The design of their technology was based on glucose oxidase- enzyme layer- entrapped within a semipermeable dialysis layer which was placed on the oxygen electrode. Following this, the first glucose analyzer was launched in 1975 which was based on Clark's technology(12). Such remarkable initiative opened up a new era in research and development centered on biosensing technologies. Since then, numerous attempts to improve the biosensing performance of such bio-devices have been studied including nanomaterials (13, 14), redox probes (15, 16), polymers (17, 18), *etc.* Furthermore, the challenge arising from the nature of the enzyme has lead researchers to search for alternative methods for glucose detection. Enzyme free glucose sensing in the presence of a catalyst is one of the most successful alternative which is capable of direct electro-oxidation of glucose. Several nanomaterials with various morphologies have been deployed as catalyst towards glucose. Among them copper based nanostructures are the most commonly used catalysts for glucose electro-oxidation due to their low-cost, narrow band gap and easy-preparation methods (11, 19-22).

Dopamine is one of the essential neurotransmitter in central nervous system and the abnormal concentration level of dopamine can be associated with several neurological disorders such as Parkinson's disease, Schizophrenia and attention deficit hyperactivity disorder (ADHD) (23). Dopamine is also a biomarker of certain cancer strains including neuroblastoma (24) and paraganglioma (25). The conventional methods for dopamine determination are high performance liquid chromatography (HPLC) (26), enzyme-linked immunosorbet assay (ELISA) (27) and capillary electrophoresis (28). Such methods can be expensive, time consuming and also those methods require specialized laboratory equipment (29). Electrochemical detection of dopamine can be an excellent alternative to current methods with low cost and rapid testing. Since dopamine is an electroactive compound which can be oxidized to dopamine-o-quinone as a reversible reaction upon application of a suitable potential. Therefore, the direct measurement of dopamine concentration by measuring the current associated with this reversible reaction is possible.

In this study, we explain the fabrication and characterization of a do-it-yourself laser scribed electrode which requires a simple laser engraving system equipped with a 405 nm wavelength laser and we also demonstrate the use of prepared electrode as sensing probe in the presence of copper/copper oxide nanostructures allowing effective detection of dopamine and glucose. We have shown here that the such nano-deposits lead to a shift of the oxidation potentials of the dopamine and ascorbic acid, thus allowing simultaneous detection of the dopamine in the presence of interference. The surface of LSE

was modified with copper nanostructure *via* electrodeposition process at negative over potentials, so called LSE-Cu. Developed LSE-Cu electrodes were used for dopamine detection in the presence of ascorbic acid. Furthermore, we have shown the use of LSE-Cu electrodes as enzyme free glucose sensors with excellent reproducibility. As we show, fabrication of LSE-Cu electrodes based dopamine and/or glucose sensors provide an inexpensive detection platform with high sensitivity and reproducibility. Noteworthy, being cost-effective and having very flexible design capabilities, such systems could be easily miniaturized into a chip platform

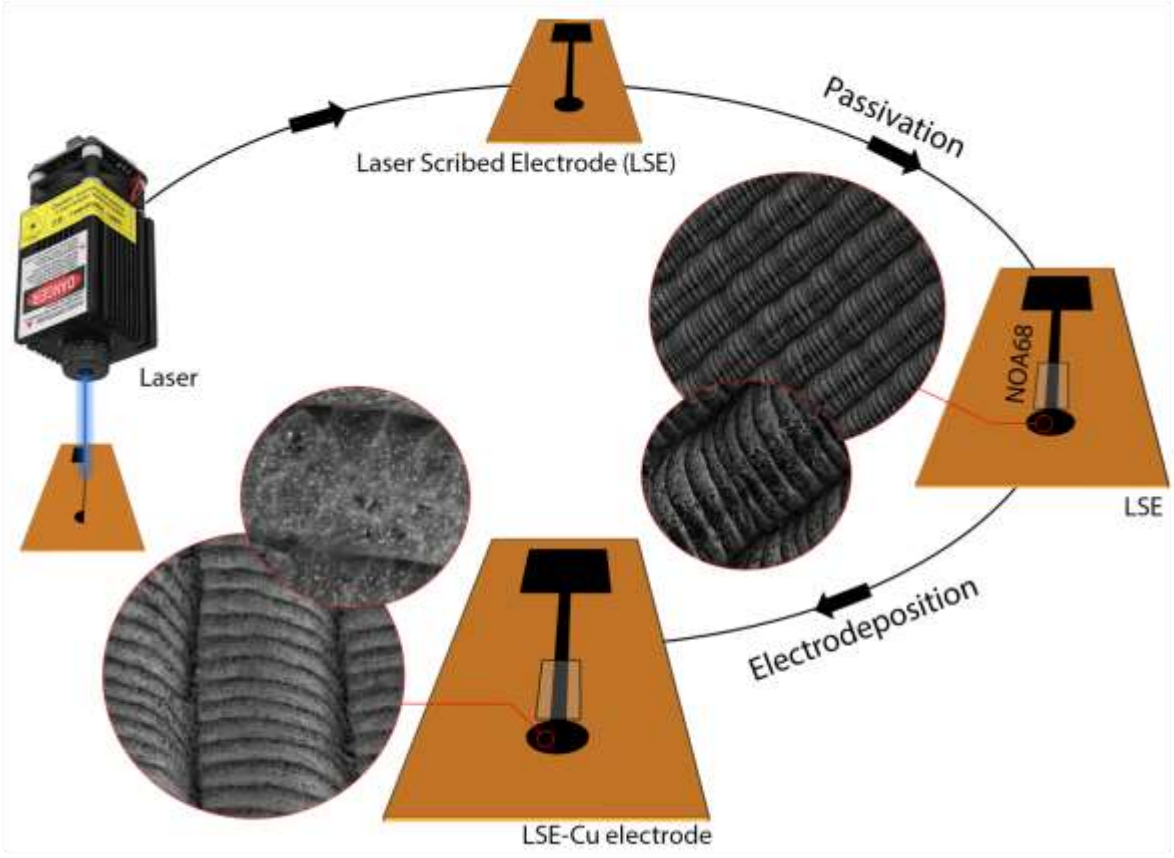

Scheme 1. Illustration of the LSE and LSE/Cu electrodes fabrication process

Materials and Methods

Chemicals and instrumentation

Copper(II) chloride dihydrate ($CuCl_2 \cdot 2H_2O$), dopamine, glucose, ascorbic acid, potassium ferrocyanide ($K_4[Fe(CN)_6]$), potassium ferricyanide ($K_3[Fe(CN)_6]$), hexaammineruthenium (III) chloride $[Ru(NH_3)_6]^{3+}$,

phosphate buffer saline tablets (PBS, 0.01 M, pH7.4), sodium hydroxide (NaOH) and potassium chloride (KCl) were obtained from Sigma-Aldrich. All solutions were prepared with double distilled and deionized water (18.3 MΩ, ELGAPurelab Ultra). Electrochemical measurements were performed on an Autolab electrochemical workstation (Metrohm, UK) equipped with a conventional 3- electrode setup consisting of a laser scribed electrode (a working electrode), a spiral Pt wire counter electrode, and a Ag/AgCl (1 M KCl) reference electrode. The surface morphology and the nanostructure of the bare and modified electrodes were studied by scanning electron microscopy (SEM) (Zeiss Supra 40 SEM at accelerating voltages in the range of 5−10 kV). The surface chemical composition of the LSE and LSE/Cu electrodes was characterized by using an X-ray photoemission spectrometer (XPS, Kratos AXIS ULTRA) with mono Al Kα radiation at 1486.58 eV; 300 W (20 mA, 15 kV). All the XPS data were calibrated by the carbon 1s peak at 284.8 eV. The energy dispersive X-ray analyses (EDX) were studied by using an SEM Quanta 650 Field Emission Gun (FEG) attached with an EDX unit, with accelerating voltage of 20 kV. The structural analysis of the LSE nano-flakes was performed by applying the transmission electron microscopy (TEM, Jeol 2100); 200 kV using a single tilt sample holder.

Fabrication of Laser Scribed electrodes, LSE

LSEs were fabricated on a polyamide film (Kapton) of 0.08 mm thickness by irradiating with a 405 nm wavelength laser in an air environment at room temperature. The continuous-wave laser with a nominal power of 0.5 W was driven by a 1 kHz, 3% duty cycle signal. The resulting optical power trace was composed of a train of exponentially decaying (τ≈0.5 ms) pulses (Supporting Information, Fig. S1). Laser has been focused to a ~50 μm diameter size spot, which was guided at the speed of 500 mm/min over the surface of the film by 2 stepper motors controlled by a conventional Grbl controller. A single exposure with the given parameters was found to be the optimal to ensure the continuity of a graphitic carbon layer with the lowest resistance (Supporting information, Fig. S2). Such low cost systems or components for assembly are easily available from the usual consumer-product online retailers.

The LSEs were designed to be of 20 mm length with a connection pad on one end, and a 2 mm diameter circular area as a working electrode on the other. Working electrode area has been isolated from the connection pad by a NOA68 ultraviolet light sensitive adhesive dispensed through a 34G needle and cured under the UV light-emitting-diode.

Electrochemical measurements

Electrodeposition of copper nanostructures was carried out by applying chronoamperometry in a solution of 40 µg / 10 mL $CuCl_2$ at a potential of – 2 V for 120 seconds. Prior to each electrodeposition process, the electrochemical cell was preconditioned for 5 s at 0 V. After electrodeposition electrodes were rinsed with double distilled water and dried in air. Electrodes were freshly prepared and used. Cyclic voltammetry of electrode were performed in a solution of 5 mM $[Fe(CN)_6]^{4-/3-}$ or in a solution of 5 mM $[Ru(NH3)_6]^{3+}$ as redox mediators in 0.01 M PBS (pH 7.4) containing 0.1 M KCl. Differential pulse voltammetry for dopamine detection was applied in 0.01 M PBS (pH 7.4), chronoamperometry for glucose detection was applied in 0.1 M NaOH solution.

Results and Discussions

Scanning electron microscopy (SEM) is one of the techniques used in here to describe the morphological features of laser scribed paths on a Kapton film. Fig.1a shows the circular working electrode surface with a diameter of 2 mm. White arrows indicate the beginning of the passivation layer of the UV curable polymer placed on the connection path. With an applied higher magnification to the surface of laser irradiated area (Fig.1b, c), highly elegant and very well-ordered laser scribed paths are clearly shown with a width of ~52 µm from top view of the sample. Fig.1c exhibits further morphological details of a single path. As it can be seen, each path consists of accordion-like successive porous segments with a width of 7 µm. The specific periodic structure arises due to the laser frequency (1 kHz) and writing speed (500 mm/min) used. Every segment is created during the peak laser exposure and partially overlaps with a several previous ones creating a continuous path overlapping with the adjacent ones. To investigate the thickness of the segments (Fig. 1 d, and e), a 30 µm-length-cut was obtained via Focused Ion Beam (FIB) at the edge of the sample. Fig. 1e shows the FIB cut at the edge of the sample and demonstrates a symmetrically curved surface of the electrode. The cross section image of the FIB cut provides a very clear image of the porous view of the laser scribed path and the sheet-like structure of thin layers (Fig. 1d). Because of the laser scribing process carried out in an air environment (in the presence of local oxygen and moisture), and because of the laser beam induced high local temperatures (>2500 C°), the carbonization and graphitization process may create *in situ* bubbles which provide a highly porous nature during the accumulation of the sheet-like thin layers(7, 30). SEM images of the LSE surface from

the top view and cross-section reveal not only the porous nature of the LSE but also the curved shape of the each path.

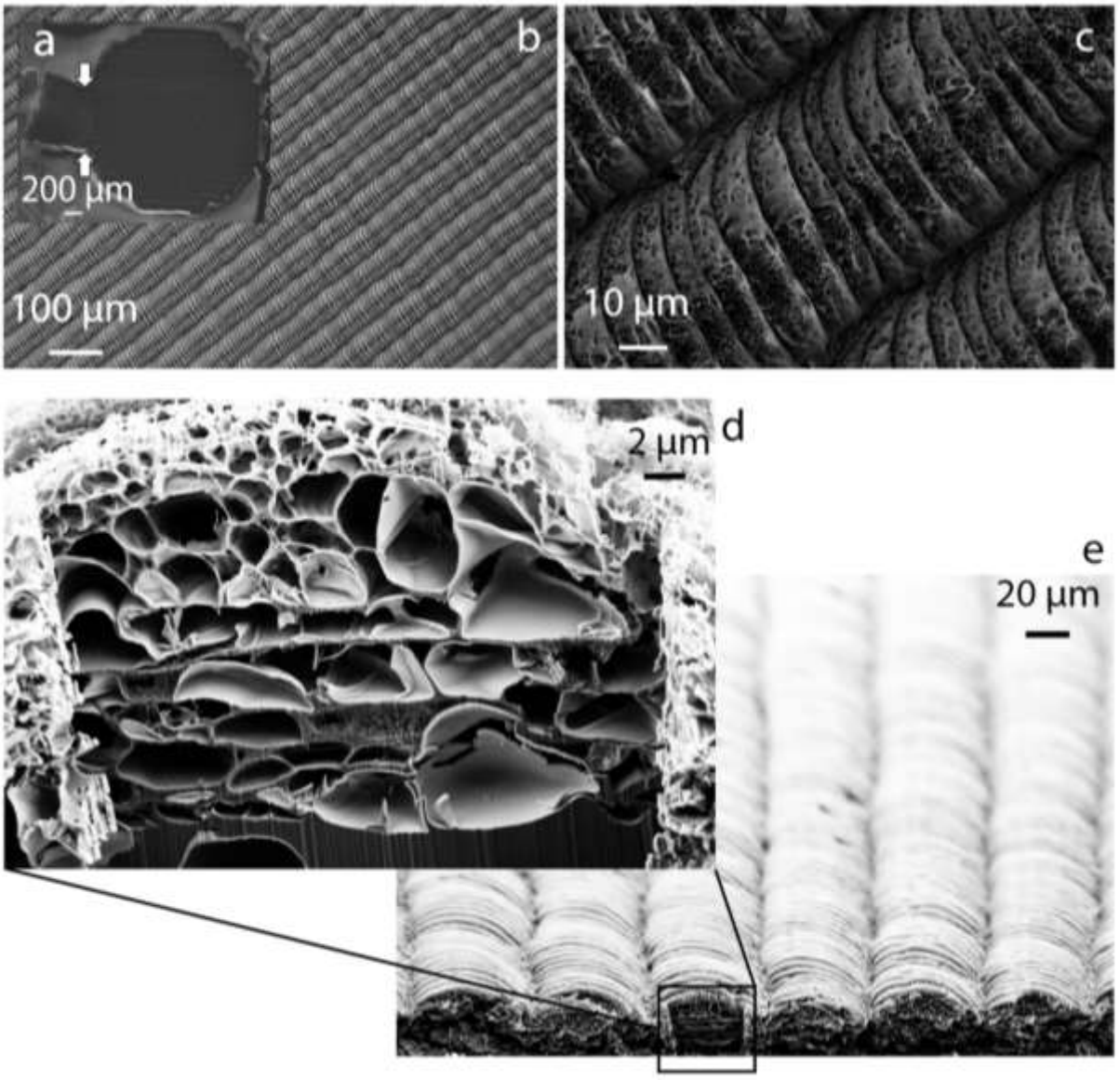

Figure 1. SEM image of the 2 mm diameter LSE (a), top view images of the LSE surface with high magnifications (b and c), single laser scribed path (d), SEM image of the cross-section of LSE surface with a FIB cut (e) and high magnification image of FIB cut cross-section (f)

Electrochemical characterization of the LSEs was studied with cyclic voltammetry in two different redox mediators. The cyclic voltammograms (CVs) of LSEs were recorded in a solution of 5 mM $[Fe(CN)_6]^{4-/3-}$ (inner sphere redox mediator) and in a solution of 5 mM $[Ru(NH3)_6]^{3+}$ (outer sphere redox mediator), respectively. Fig. 2 a and b show the voltammograms of LSEs repeated with three different electrodes. In

both systems electrodes showed highly reproducible voltammograms and peak currents with relative standard deviations of 5.52 % and 2.44 % in mM $[Fe(CN)_6]^{4-/3-}$ and $[Ru(NH3)_6]^{3+}$, respectively. The peak separation (ΔE_p) of LSE in $[Fe(CN)_6]^{4-/3-}$ is determined to be 289.3 mV, however electrodes showed smaller ΔE_p value of 179.7 mV in a solution of $[Ru(NH3)_6]^{3+}$. Since the surface of the LSE fabricated here is highly porous and consisted of several different states of carbon, it is expected that the surface sensitive redox reaction of $Fe^{3+/2+}$ may provide a higher value of ΔE_p. However, a lower ΔE_p of $[Ru(NH3)_6]^{3+}$ indicates a faster heterogeneous electron transfer due to the surface insensitive nature of the redox probe. The electrode kinetics was further studied with three different LSEs at different scan rates for both redox probes. Fig. 2 c and d shows the resulting voltammograms of the electrodes and inset graphs show the corresponding graphs of square root of scan rate vs. peak current. The redox reactions appear to be quasi-reversible resulting in a linear increase of the peak current with increased square root of scan rate. This may be attributed to the diffusion controlled voltammetry of both redox systems which allowed to study the heterogeneous standard rate constant (k^0) by using a well-known kinetic parameter of Nicholson theory(31):

$$\Psi = k^0 (\frac{\pi D n v F}{RT})^{-1/2}$$

where Ψ is the dimensionless kinetic parameter, D is the diffusion coefficient of the electroactive species, v is the scan rate, F is the Faraday constant, R is the universal gas constant, and T is the absolute temperature.

Lavagnini *et al*(32) defined the following equation by extending the Nicholson theory from the curve of Ψ vs. ΔE_p x n; where X indicates ΔE_p x n:

$$\Psi = \frac{-0.6288 + 0.0021X}{1 - 0.017X}$$

Thus the kinetic parameter k^0 may be easily evaluated from the slop of the plots of Ψ vs. $[\pi DnF\ (RT)]^{-1/2} v^{-1/2}$, which were shown in Supporting Information, Fig. S3. The average k^0 value of the LSEs studied in $[Fe(CN)_6]^{4-/3-}$ is calculated to be 0.025 cm s^{-1} and for $[Ru(NH3)_6]^{3+}$ the calculated average value is 0.065 cm s^{-1}. Those values are better than many other values of carbon based surfaces available in the literature. For instance the k^0 value of graphene on copper electrodes(33) was reported to be 0.014 cm

s^{-1} for potassium ferrocyanide (II) and 0.012 cm s^{-1} for hexaammineruthenium (III) chloride. The k^0 value of the DVD-Laser scribed graphene electrode(5) was calculated to be 0.02373 cm s^{-1} for potassium ferricyanide. The k^0 values of monolayer-graphene and quasi-graphene(34) were determined to be 0.00111 and 0.00158 cm s^{-1} , respectively for $Ru(NH_3)_6^{3+/2+}$.

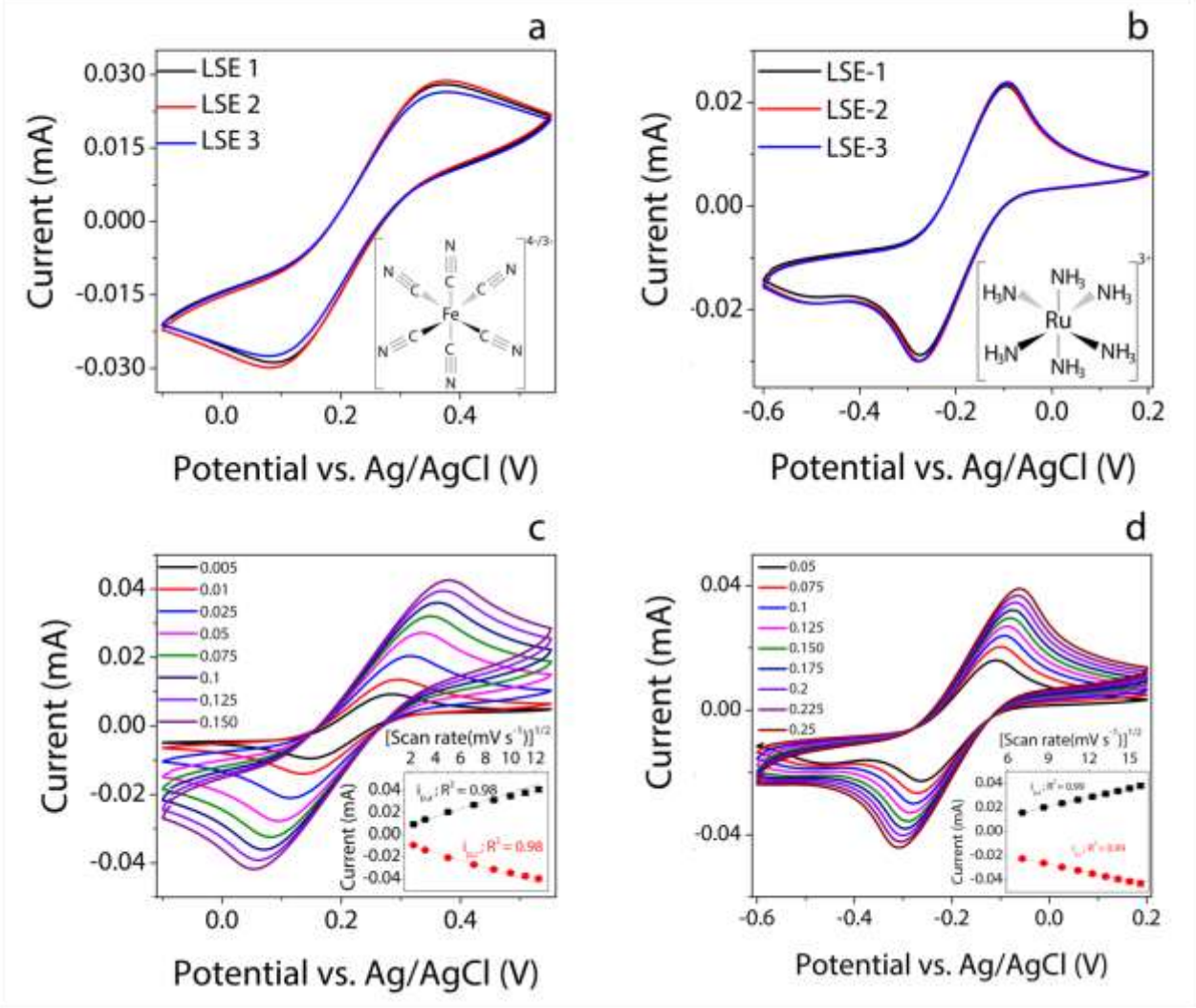

Figure 2. Cyclic voltammograms recorded with three individual LSEs; the solution is 5 mM $Fe(CN)_6^{3-/4-}$ as a redox probe in 0.01 M PBS (pH 7.4), containing 0.1 M KCl (a), the solution is 5 mM $Ru(NH_3)_6^{3+/2+}$ as a redox probe in 0.01 M PBS (pH 7.4), containing 0.1 M KCl, Cyclic voltammograms recorded with three individual LSEs at the scan rates ranging from 0.005 to 0.150 V s^{-1} in 5 mM $Fe(CN)_6^{3-/4-}$ redox probe (inset: corresponding I-$v^{1/2}$ graph) (c) and cyclic voltammograms recorded with three individual LSEs at the scan rates ranging from 0.05 to 0.25 V s^{-1} in 5 mM $Ru(NH_3)_6^{3+/2+}$ redox probe (inset: corresponding I-$v^{1/2}$ graph) (d)

The chemical structure was studied by energy dispersive X-Ray Analysis (EDX). Fig. 3a shows the EDX analysis and corresponding SEM mapping image of the analysis. The carbon appears in red color which covers the entire surface of the analysis area with the ratio of 100%.

The structural morphology of the LSE flakes was further analyzed with transmission electron microscopy (TEM). Fig. 3b shows the TEM image of the LSE flakes which were dispersed in double distilled water by ultrasonicating and drop casted onto a copper grid with a Lacey C. TEM image demonstrates the sheet-like appearance of the LSE flakes with a thickness of a few layers and the existence of the graphite phase and amorphous regions.

Fig. 3c shows material analysis obtained by Raman spectroscopy (532 nm laser, spot size ~2 µm). Typical spectra with three dominant characteristic peaks at 1345 cm^{-1}, 1570 cm^{-1} and 2675 cm^{-1}, conventionally referred to as bands D, G and 2D, respectively, were observed(35). The presence of G and 2D bands is typically associated with graphene and graphite, where a well expressed 2D peak indicates high quality graphene(36). The D band is very often attributed to the disorder of the layers – edge defects would be an example. High intensity and the broadening of this peak clearly indicate a disordered nature of our electrodes. To check the uniformity, several adjacent points have been probed (Fig. 3c). The obtained Raman scattering spectra are dominant by the same peaks, however, of a different intensity and broadening confirming non-uniform morphology and composition of carbonized areas. We would like to stress that, while during the quest of high quality graphene many researchers tend to emphasize the fact of the graphene presence, we want to show that this is not essential and various disordered graphitic carbon species can form substrates highly suitable for practical applications.

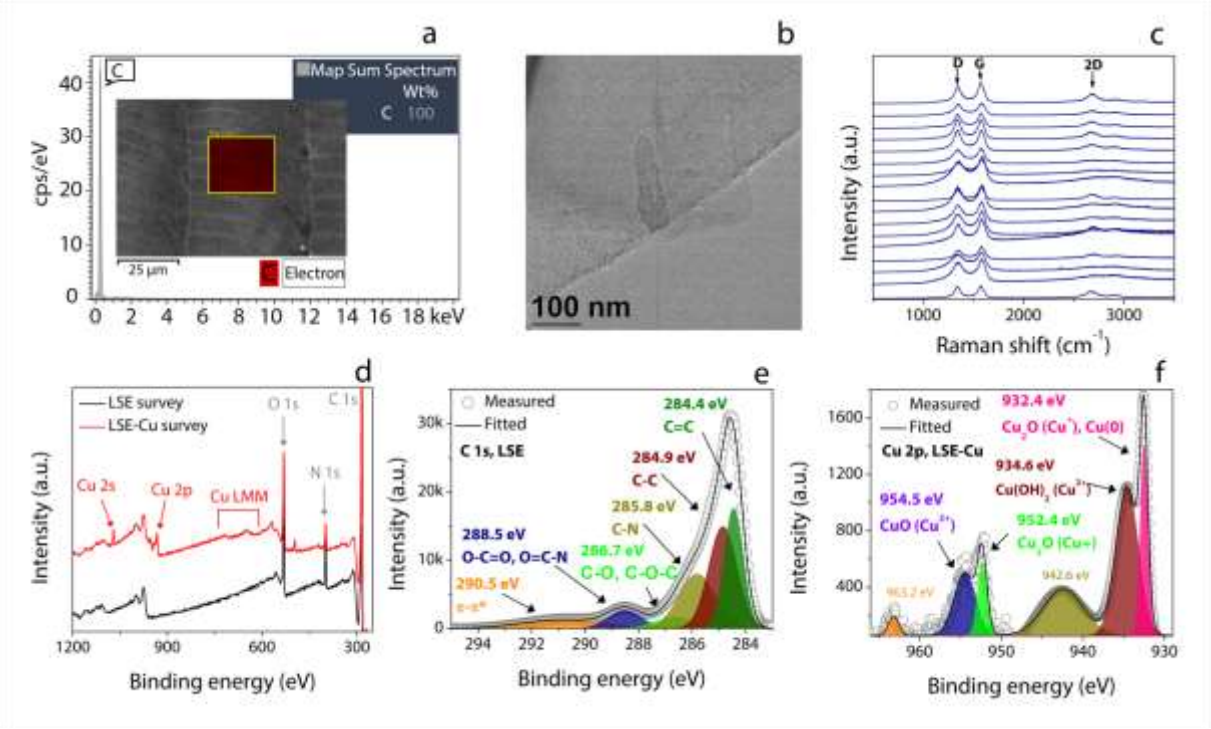

Figure 3. EDX spectra of LSE surface (insets; SEM image, EDX mapping analysis, and Map Sum spectrum) (a), TEM image of LSE flakes (b), Raman spectra of LSE surface of different LSEs and regions (c), XPS survey scans of LSE and LSE-Cu surfaces (d), C 1s XPS spectra of LSE (e), and Cu 2p XPS spectra of LSE-Cu surface (f)

The as-prepared LSEs were modified with copper nanostructures via electrodeposition process. The effect of the applied voltage onto electrodeposition process of copper was studied to determine the optimum electrodeposition condition. Supporting information, Fig. S4 shows the SEM images of LSE/Cu electrodes which were prepared at applied voltages of -4 V (a, and b), -3 V (c) and -1 V (d). The deposition process at -4 V resulted in high accumulation of the Cu nanostructures, such high negative voltage lead the growth of the dendritic Cu nanostructures at the edges of the segments on the laser path (Supporting information, Fig. S4a). Furthermore, the dendritic growth was observed at the edges of the each laser path (Supporting information, Fig. S4b). Decreased deposition voltage resulted in decreased Cu nanostructure concentration on the surface. The applied potential of – 3 V showed more uniform surface deposition however the best deposition condition was obtained at -2 V. The applied deposition potential of -1 V provided the lowest accumulation of nanostructures.

The surface chemical composition of LSE and LSE-Cu electrodes were characterized by XPS. Fig. 3d shows the measured survey scans of the both electrodes' surfaces, which shows the existence of the carbon, oxygen and nitrogen as joint elements. High resolution spectra of C 1s from LSE (Fig. 3e) reveal clearly that indeed the main peaks of C=C (sp^2, 284.5 eV) and C-C (sp^3, 284.9 eV) carbon bonds are present on the surface. The peaks of the C-N at 285,8 eV and O=C-N at 288.5 eV are most likely the contributions from the Kapton film(30). The XPS survey of LSE-Cu confirms the presence of the Cu on the surface, Fig.3d. The high resolution Cu 2p XPS spectrum of LSE-Cu surface is shown in Fig.3f. The main peaks located at ~932.4 and 934.6 eV are attributed to the existence of Cu_2O, Cu^0 and $Cu(OH)_2$. The peaks at ~952.4 and 954.5 eV were assigned to CuO and Cu_2O, respectively(37, 38). The detailed analysis of Cu 2p from LSE-Cu reveals clearly that the composition of copper electrodeposits are consisted of a mixture of the copper and copper-oxide species(37).

Fig. 4a and b show the SEM images of the LSE after copper nanostructures deposition. The homogenous distribution of copper nanostructures on the surface of the LSE was shown with a series of the SEM images from low to high magnifications. EDX spectra with mapping analysis of Cu nanostructures deposited LSE is shown in Fig.4c. The copper appears in pink color on the surface of the analysis area with a ratio of 0.3%. We note that this measurement is merely a qualitative one clearly indicating the existence of Cu nanostructures on the electrode surface. Due to the limitation of the SEM-EDX with these specific samples at different applied operation voltages, real concentrations could not be measured by this method. The structural morphology of LSE/Cu flakes was determined by TEM. Fig. 4 d and e show the TEM images of the Cu deposited flakes. The TEM images of the LSE/Cu graphitic layers with darker spots darker regions confirm the presence of the copper nanostructures.

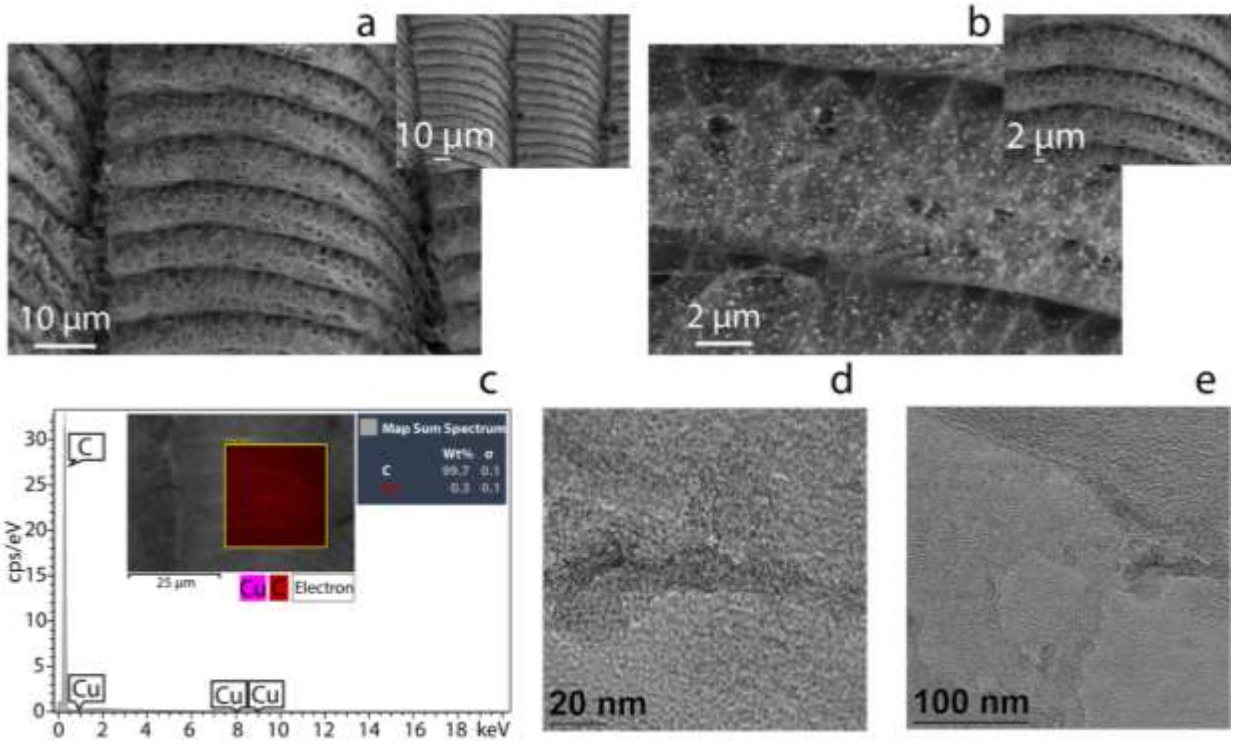

Figure 4. SEM images of LSE/Cu laser path at low and high magnifications (a), high magnification SEM images of Cu nanostructures deposited surface of LSE (b) EDX spectra of LSE/Cu surface (insets; SEM image, EDX mapping analysis, and Map Sum spectrum), and TEM images of LSE/Cu flakes (d and e)

The LSE and LSE/Cu electrodes were used for electrochemical oxidation of dopamine in the presence of ascorbic acid in 0.01 M PBS (pH 7.4). Dopamine is an electroactive compound and the oxidation of dopamine can be achieved at a certain applied potential (39-41). Since the ascorbic acid displays redox behavior at potentials close to the oxidation potential of dopamine, LSEs were modified with copper nanostructures to overcome such problem by altering the electrode kinetics of both dopamine and ascorbic acid(42). Therefore, a shift was obtained at the oxidation potential of the target species which allowed the detection of dopamine in the presence of chosen interfering molecule of ascorbic acid. For this purpose, firstly the sensing potential of the electrodes were investigated by CV. Fig. 5 shows the CV performances of LSE (a, b and c) and LSE/Cu (d, e and f) electrodes in the absence and presence of dopamine and/or ascorbic acid. The CV of the LSE in PBS (Fig. 5a, black) has no obvious peak, however in the presence of the ascorbic acid and dopamine well-defined peaks appear at 0.018 V and 0.206 V. The oxidation of the dopamine itself via LSE is observed at ca. 0.19 V (Fig. 5b) and the oxidation of ascorbic acid at LSE surface appears as a very broad peak between ca. -0.06 V and 0.48 V (Fig. 5c) which overlaps with the dopamine oxidation peak potential. Therefore the resulting peak current of dopamine in the

presence of ascorbic acid at 0.206 V provides a false recording due to overlapping oxidation potentials of both species. The same conditions were studied with LSE/Cu electrodes in order to investigate the benefit of the copper nanostructures on the electrode surface for dopamine catalysis. Fig. 5d shows the CV of LSE/Cu electrode in the presence of ascorbic acid and dopamine. The LSE/Cu electrode showed higher current level toward dopamine with a well-defined peak shape and the oxidation potential of dopamine shifted positively to 0.232 V (Fig. 5e). Furthermore, as shown in Fig. 5f, the oxidation potential of ascorbic acid appears as a peak at ca. 0.093 V. Overall, the oxidation peak separation of ascorbic acid and dopamine is 199 mV at LSE whereas the separation is 231 mV at LSE/Cu electrode. Thus selective and simultaneous determination of dopamine is demonstrated via LSE/Cu electrodes in the presence of ascorbic acid.

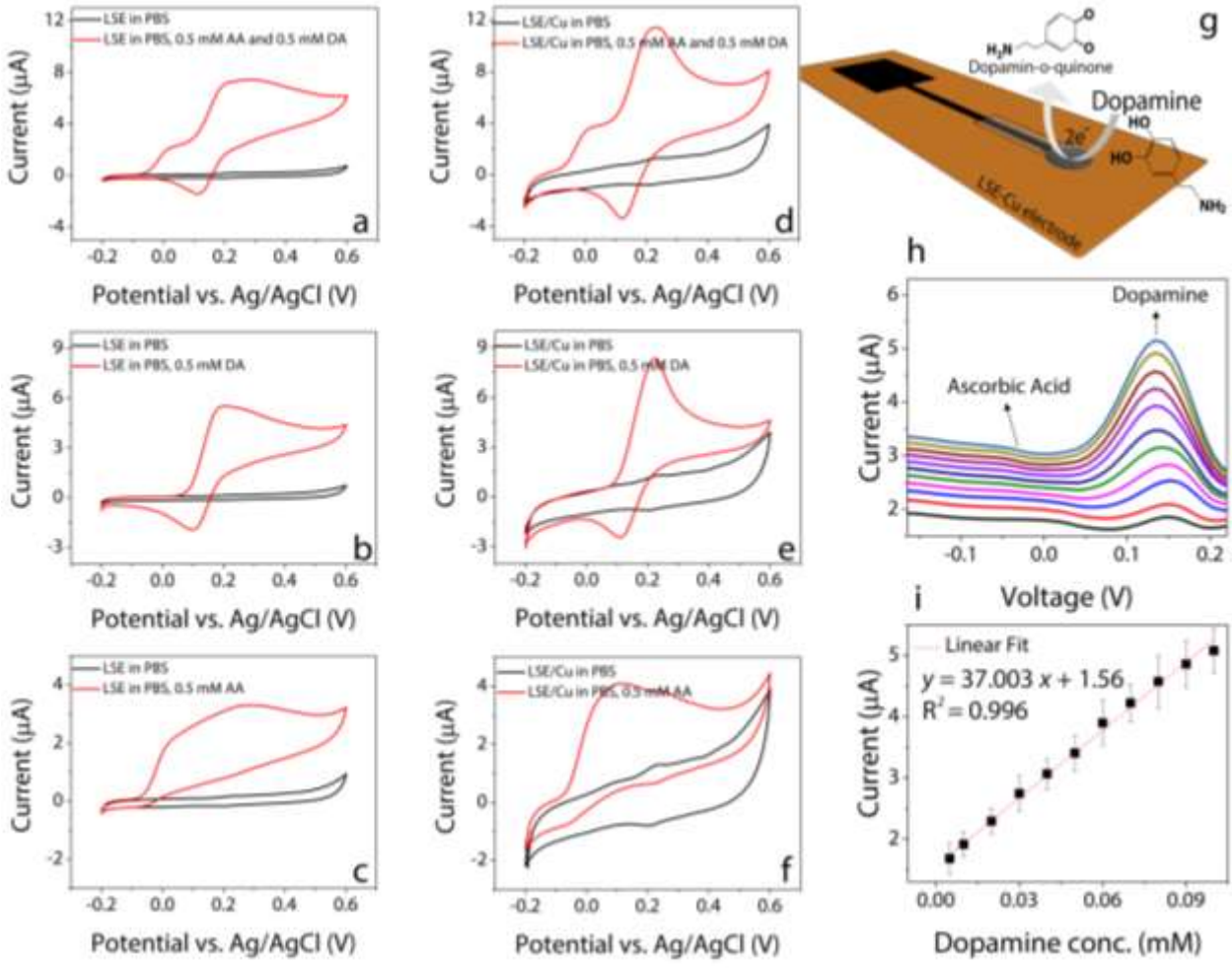

Figure 5. CVs of LSEs in the absence and presence of (a) 0.5 mM AA and 0.5 mM DA, (b) 0.5 mM DA, and (c) 0.5 mM AA in 0.01 M PBS (pH 7.4). CVs of LSE/Cu electrode in the absence and presence of (d) 0.5

mM AA and 0.5 mM DA, (e) 0.5 mM DA, (f) 0.5 mM AA in 0.01 M PBS (pH 7.4), (g) Schematic representation of the dopamine oxidation mechanism on LSE/Cu electrode surface, (h) DPV response of LSE/Cu electrode toward increased concentrations of dopamine and ascorbic acid, (i) Corresponding calibration curve of LSE/Cu electrode for dopamine sensing

Fig. 5g shows the schematic image of the dopamine electro-oxidation mechanism on the surface of LSE/Cu electrode. Using the differential pulse voltammetry (DPV), we carried out the concentration studies of dopamine. Fig. 5h exhibits the DP voltammograms of each studied concentration and Fig. 5i shows the corresponding calibration curve of LSE/Cu sensor towards dopamine. Developed LSE/Cu sensor exhibits a linear region the range of concentrations between 0.005 mM and 0.1 mM. The fitting equation is $I\ (\mu A) = 37.003\ [C_{dopamine}](mM) + 1.56$ with a correlation coefficient of 0.996 (R^2). The sensitivity of the LSE/Cu sensor toward dopamine was determined to be 1321.54 μA mM^{-1} cm^{-2}. LSE/Cu sensor exhibited en excellent performance in terms of the sensitivity of the developed sensor for dopamine electro-detection. This result clearly reveals the great advantage of the laser scribed electrode platform as bio-sensing component. Furthermore, the reproducibility of the LSE/Cu electrode was also studied. For this purpose four individual LSE/Cu sensors were prepared and applied for dopamine detection under the same conditions. Resulting current densities were used to calculate the relative standard deviation which was determined to be 9.32% (RSD %). High sensitivity and the reproducibility of the LSE/Cu sensor show high robustness of the developed laser scribed electrodes.

The LSE and LSE/Cu electrodes were further used to investigate the glucose electro-oxidation in alkaline environment. Fig. 6a,b show the electrochemical behavior of the LSE based electrodes in 0.1 M NaOH solution in the absence and the presence of glucose. As it can be seen in Fig. 6a, the LSE shows a weak and broad glucose oxidation peak at around -0.27 V. Fig. 6b shows the electrochemical behavior of the LSE/Cu electrode in alkaline solution and Fig. 6c shows the CV of LSE/Cu electrode in detail. In the anodic sweep of the CV a series of subsequent multiple peaks (from ca. -0.4 V to +0.3 V) are observed due to formation of the copper oxide species on the electrode surface(37). The subsequent reduction of the oxide species appeared in the cathodic sweep of the CV at a potential of 0 V and at a potential of – 0.5 V. After the addition of glucose, a peak around 0.45 V vs Ag/AgCl appears while there is no obvious peak at the same potential in the absence of glucose in Fig. 6b. The most accepted explanation for the glucose electro-oxidation mechanism in alkaline solution shown below is the formation of the Cu(III) oxides such as CuOOH. In the anodic sweep during the CV scan copper oxides form on the electrode

surface, and a further oxidation of those species to Cu^{3+} may occur. This is followed by the reduction in the cathodic sweep to Cu(II)(37, 43-45):

$Cu(II) \rightarrow Cu(III) + e^-$

$Cu(III)\ 4\ OH^- \rightarrow Cu(II) + 2H_2O + O_2$

Cu(II)-glucose → Cu(III)-glucose → Gluconolactone + Cu(II)

Since the aim of the present work was to study the oxidation of glucose, +0.45 V was selected as the applied oxidation potential for glucose sensing in alkaline environment at the surface of LSE/Cu electrodes.

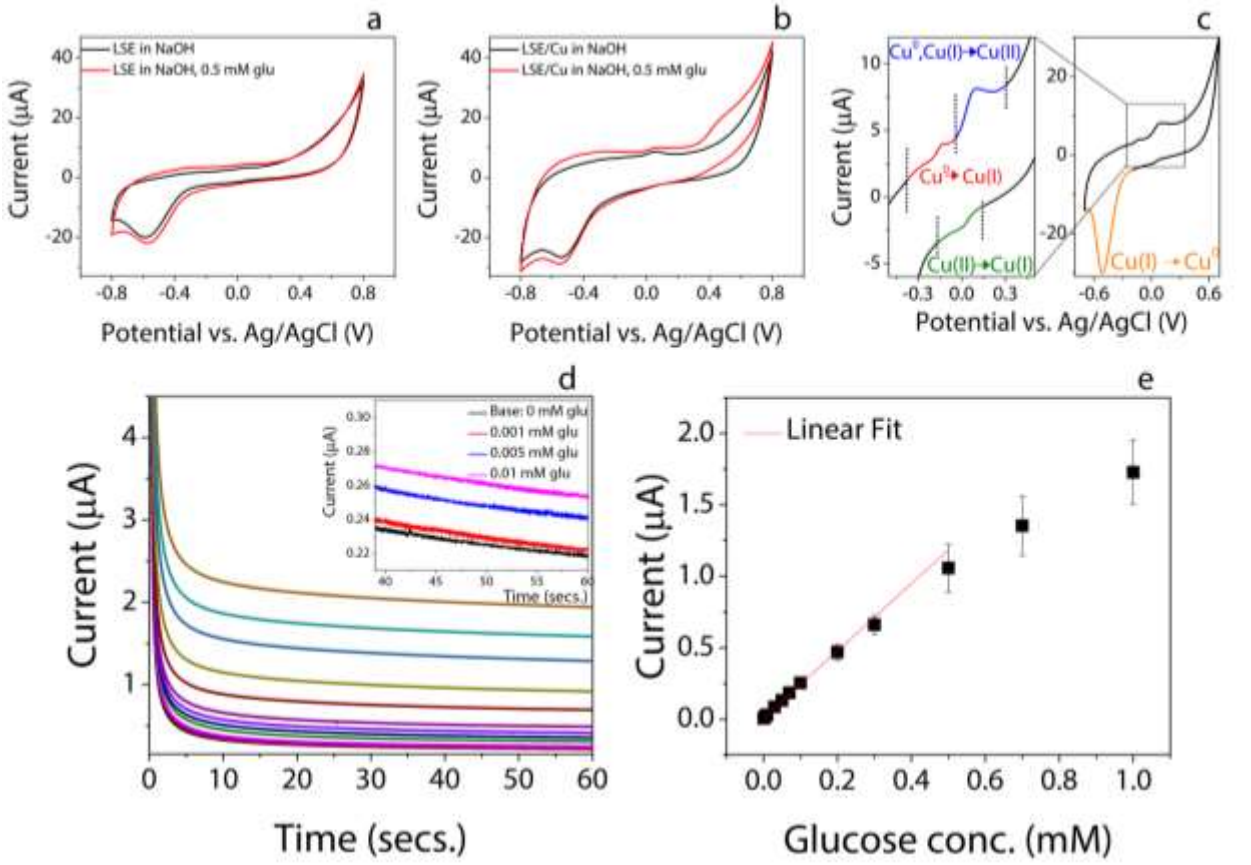

Figure 6. CVs of LSE (a) and LSE/Cu (b) electrodes in 0.1 M NaOH solution in the absence and presence of glucose.

Fig. 6d displays the chronoamperograms obtained by using the LSE/Cu electrode at an applied potential of +0.45 V and the inset shows the magnified section of amperograms between the 40th and 60th

seconds belong to the base line and the first three applied concentrations of glucose(46). Chronoamperometry was studied with LSE/Cu electrodes as a function of increased concentrations of glucose in 0.1 M NaOH solution at room temperature under non-stirred conditions. Each concentration was applied in a freshly prepared glucose concentration in NaOH solution and measured immediately. As it can be seen LSE/Cu electrodes reach steady state current level very quickly, therefore the current values obtained at 60th seconds were used to evaluate the sensitivity of the LSE/Cu sensor. Fig. 6e demonstrates the corresponding calibration curve of the LSE/Cu sensor towards glucose with a linear region in the range of concentrations between 0.001 mM and 0.5 mM. The regression equation of LSE/Cu sensor is $I(\mu A)=2.355[C_{glucose}](mM) + 0.007$ with a correlation coefficient of 0.99. The sensitivity of the LSE/Cu sensor was determined to be 84.07 μA mM^{-1} cm^{-2}. The obtained satisfying sensitivity of the LSE/Cu sensor towards glucose demonstrates that the laser scribed electrodes may provide cheap and sensitive electrochemical detection platform towards varying analytes. Previously we have reported the effect of the concentration of the copper nanostructures on the performance of the glucose-electro-oxidation(37). Since the sensitivity of the copper nanostructures based platforms are mostly depended on the concentration of the accumulated copper species on the electrode surface, it is highly possible to improve the sensitivity of the proposed LSE/Cu sensor here towards glucose electro-oxidation. The response reproducibility of the LSE/Cu sensor towards the glucose was further investigated. Four as-prepared samples of LSE/Cu were tested towards glucose by applying the same conditions of chronoamperometric measurements, and the relative standard deviation of the recorded current densities was calculated to be 5.47 % (RSD %). This statistical value of the LSE/Cu sensor demonstrates the high degree of reproducibility of the developed electrode.

Conclusions

Recent advancements show that laser scribed electrodes (LSEs) are becoming a very solid, low-cost alternative for the conventional carbon based electrodes. A clear trend of an increasing interest in this group of electrodes has been lately observed in the field of electrochemical biosensors. Thus in this study we provide a simple design, fabrication and passivation route for the preparation of the LSEs performing as biosensors. The morphological, elemental and electrochemical analysis of the electrodes was studied in detail by SEM, EDX, XPS, TEM and CVs with inner and outer sphere mediators. The fabricated LSEs were modified with Cu/Cu-oxide nanostructures. The application of the Cu/Cu-oxide nanostructures allowed the discrimination of the oxidation peak of the dopamine in the presence of the interfering specie of ascorbic acid by shifting the peak potential – one of the key demonstrations in this

work. Thus the developed system provided excellent performance towards dopamine oxidation. Furthermore, LSE-Cu electrodes were used for glucose electrode-oxidation since copper is one of the most popular glucose catalyst. The obtained results demonstrated high reproducibility of the sensing platform for glucose detection. Noteworthy the laser scribing process provides flexibility of the design of the electrodes and such electrodes are highly suitable for further miniaturization and packaging.

Acknowledgements

This work was partially supported by Internal Catalyst Grant, ICA1920 in Tyndall National Institute, Cork, Ireland.

References

1. Lawal AT. Progress in utilisation of graphene for electrochemical biosensors. Biosensors and Bioelectronics. 2018;106:149-78.
2. Ratinac KR, Yang WR, Gooding JJ, Thordarson P, Braet F. Graphene and Related Materials in Electrochemical Sensing. Electroanalysis. 2011;23(4):803-26.
3. Fenzl C, Nayak P, Hirsch T, Wolfbeis OS, Alshareef HN, Baeumner AJ. Laser-Scribed Graphene Electrodes for Aptamer-Based Biosensing. ACS Sensors. 2017;2(5):616-20.
4. El-Kady MF, Strong V, Dubin S, Kaner RB. Laser Scribing of High-Performance and Flexible Graphene-Based Electrochemical Capacitors. Science. 2012;335(6074):1326-30.
5. Griffiths K, Dale C, Hedley J, Kowal MD, Kaner RB, Keegan N. Laser-scribed graphene presents an opportunity to print a new generation of disposable electrochemical sensors. Nanoscale. 2014;6(22):13613-22.
6. Lin J, Peng Z, Liu Y, Ruiz-Zepeda F, Ye R, Samuel ELG, et al. Laser-induced porous graphene films from commercial polymers. Nature Communications. 2014;5(1):5714.
7. Nayak P, Kurra N, Xia C, Alshareef HN. Highly Efficient Laser Scribed Graphene Electrodes for On-Chip Electrochemical Sensing Applications. Advanced Electronic Materials. 2016;2(10):1600185.
8. Lin S, Feng W, Miao X, Zhang X, Chen S, Chen Y, et al. A flexible and highly sensitive nonenzymatic glucose sensor based on DVD-laser scribed graphene substrate. Biosensors and Bioelectronics. 2018;110:89-96.
9. Xu G, Jarjes ZA, Desprez V, Kilmartin PA, Travas-Sejdic J. Sensitive, selective, disposable electrochemical dopamine sensor based on PEDOT-modified laser scribed graphene. Biosensors and Bioelectronics. 2018;107:184-91.
10. Chyan Y, Ye R, Li Y, Singh SP, Arnusch CJ, Tour JM. Laser-Induced Graphene by Multiple Lasing: Toward Electronics on Cloth, Paper, and Food. ACS Nano. 2018;12(3):2176-83.
11. Juska VB, Pemble ME. A Critical Review of Electrochemical Glucose Sensing: Evolution of Biosensor Platforms Based on Advanced Nanosystems. Sensors (Basel). 2020;20(21).
12. Newman JD, Turner APF. Home blood glucose biosensors: a commercial perspective. Biosens Bioelectron. 2005;20(12):2435-53.
13. Buk V, Pemble ME. A highly sensitive glucose biosensor based on a micro disk array electrode design modified with carbon quantum dots and gold nanoparticles. Electrochimica Acta. 2019;298:97-105.

14. Buk V, Pemble ME, Twomey K. Fabrication and evaluation of a carbon quantum dot/gold nanoparticle nanohybrid material integrated onto planar micro gold electrodes for potential bioelectrochemical sensing applications. Electrochimica Acta. 2019;293:307-17.
15. Bilgi M, Sahin EM, Ayranci E. Sensor and biosensor application of a new redox mediator: Rosmarinic acid modified screen-printed carbon electrode for electrochemical determination of NADH and ethanol. Journal of Electroanalytical Chemistry. 2018;813:67-74.
16. Cui L, Hu J, Li C-c, Wang C-m, Zhang C-y. An electrochemical biosensor based on the enhanced quasi-reversible redox signal of prussian blue generated by self-sacrificial label of iron metal-organic framework. Biosensors and Bioelectronics. 2018;122:168-74.
17. Buk V, Emregul E, Emregul KC. Alginate copper oxide nano-biocomposite as a novel material for amperometric glucose biosensing. Materials Science & Engineering C-Materials for Biological Applications. 2017;74:307-14.
18. Juska VB, Pemble ME. A dual-enzyme, micro-band array biosensor based on the electrodeposition of carbon nanotubes embedded in chitosan and nanostructured Au-foams on microfabricated gold band electrodes. Analyst. 2020;145(2):402-14.
19. Juska VB, Walcarius A, Pemble ME. Cu Nanodendrite Foams on Integrated Band Array Electrodes for the Nonenzymatic Detection of Glucose. Acs Appl Nano Mater. 2019;2(9):5878-89.
20. Noh HB, Lee KS, Chandra P, Won MS, Shim YB. Application of a Cu-Co alloy dendrite on glucose and hydrogen peroxide sensors. Electrochimica Acta. 2012;61:36-43.
21. Liu X, Yang W, Chen L, Jia J. Three-Dimensional Copper Foam Supported CuO Nanowire Arrays: An Efficient Non-enzymatic Glucose Sensor. Electrochimica Acta. 2017;235:519-26.
22. Wang X, Ge CY, Chen K, Zhang YX. An ultrasensitive non-enzymatic glucose sensors based on controlled petal-like CuO nanostructure. Electrochimica Acta. 2018;259:225-32.
23. Shin J-W, Yoon J, Shin M, Choi J-W. Electrochemical Dopamine Biosensor Composed of Silver Encapsulated MoS2 Hybrid Nanoparticle. Biotechnology and Bioprocess Engineering. 2019;24(1):135-44.
24. Anagnoste B, Freedman LS, Goldstein M, Broome J, Fuxe K. Dopamine- -hydroxylase activity in mouse neuroblastoma tumors and in cell cultures. Proc Natl Acad Sci U S A. 1972;69(7):1883-6.
25. Eisenhofer G, Goldstein DS, Sullivan P, Csako G, Brouwers FM, Lai EW, et al. Biochemical and clinical manifestations of dopamine-producing paragangliomas: utility of plasma methoxytyramine. J Clin Endocrinol Metab. 2005;90(4):2068-75.
26. Hubbard KE, Wells A, Owens TS, Tagen M, Fraga CH, Stewart CF. Determination of dopamine, serotonin, and their metabolites in pediatric cerebrospinal fluid by isocratic high performance liquid chromatography coupled with electrochemical detection. Biomed Chromatogr. 2010;24(6):626-31.
27. Kim J, Jeon M, Paeng KJ, Paeng IR. Competitive enzyme-linked immunosorbent assay for the determination of catecholamine, dopamine in serum. Anal Chim Acta. 2008;619(1):87-93.
28. Li H, Li C, Yan ZY, Yang J, Chen H. Simultaneous monitoring multiple neurotransmitters and neuromodulators during cerebral ischemia/reperfusion in rats by microdialysis and capillary electrophoresis. Journal of Neuroscience Methods. 2010;189(2):162-8.
29. Vázquez-Guardado A, Barkam S, Peppler M, Biswas A, Dennis W, Das S, et al. Enzyme-Free Plasmonic Biosensor for Direct Detection of Neurotransmitter Dopamine from Whole Blood. Nano Letters. 2019;19(1):449-54.
30. Burke M, Larrigy C, Vaughan E, Paterakis G, Sygellou L, Quinn AJ, et al. Fabrication and Electrochemical Properties of Three-Dimensional (3D) Porous Graphitic and Graphenelike Electrodes Obtained by Low-Cost Direct Laser Writing Methods. ACS Omega. 2020;5(3):1540-8.
31. Nicholson RS. Theory and Application of Cyclic Voltammetry for Measurement of Electrode Reaction Kinetics. Analytical Chemistry. 1965;37(11):1351-+.
32. Lavagnini I, Antiochia R, Magno F. An extended method for the practical evaluation of the standard rate constant from cyclic voltammetric data. Electroanalysis. 2004;16(6):505-6.

33. Bosch-Navarro C, Laker ZPL, Rourke JP, Wilson NR. Reproducible, stable and fast electrochemical activity from easy to make graphene on copper electrodes. Physical Chemistry Chemical Physics. 2015;17(44):29628-36.
34. Brownson DAC, Varey SA, Hussain F, Haigh SJ, Banks CE. Electrochemical properties of CVD grown pristine graphene: monolayer- vs. quasi-graphene. Nanoscale. 2014;6(3):1607-21.
35. Pimenta MA, Dresselhaus G, Dresselhaus MS, Cançado LG, Jorio A, Saito R. Studying disorder in graphite-based systems by Raman spectroscopy. Physical Chemistry Chemical Physics. 2007;9(11):1276-90.
36. Silva DL, Campos JLE, Fernandes TFD, Rocha JN, Machado LRP, Soares EM, et al. Raman spectroscopy analysis of number of layers in mass-produced graphene flakes. Carbon. 2020;161:181-9.
37. Juska VB, Walcarius A, Pemble ME. Cu Nanodendrite Foams on Integrated Band Array Electrodes for the Nonenzymatic Detection of Glucose. ACS Applied Nano Materials. 2019.
38. Nam DH, Taitt BJ, Choi KS. Copper-Based Catalytic Anodes To Produce 2,5-Furandicarboxylic Acid, a Biomass-Derived Alternative to Terephthalic Acid. Acs Catalysis. 2018;8(2):1197-206.
39. Bacil RP, Chen LF, Serrano SHP, Compton RG. Dopamine oxidation at gold electrodes: mechanism and kinetics near neutral pH. Physical Chemistry Chemical Physics. 2020;22(2):607-14.
40. Pham AN, Waite TD. Cu(II)-catalyzed oxidation of dopamine in aqueous solutions: Mechanism and kinetics. Journal of Inorganic Biochemistry. 2014;137:74-84.
41. Sundar S, Venkatachalam G, Kwon SJ. Biosynthesis of Copper Oxide (CuO) Nanowires and Their Use for the Electrochemical Sensing of Dopamine. Nanomaterials-Basel. 2018;8(10).
42. Henstridge MC, Dickinson EJF, Aslanoglu M, Batchelor-McAuley C, Compton RG. Voltammetric selectivity conferred by the modification of electrodes using conductive porous layers or films: The oxidation of dopamine on glassy carbon electrodes modified with multiwalled carbon nanotubes. Sensors and Actuators B: Chemical. 2010;145(1):417-27.
43. Deng YL, Handoko AD, Du YH, Xi SB, Yeo BS. In Situ Raman Spectroscopy of Copper and Copper Oxide Surfaces during Electrochemical Oxygen Evolution Reaction: Identification of Cu-III Oxides as Catalytically Active Species. Acs Catalysis. 2016;6(4):2473-81.
44. Zheng WR, Li Y, Tsang CS, Hu LS, Liu MJ, Huang BL, et al. Cu-II-Mediated Ultra-efficient Electrooxidation of Glucose. Chemelectrochem. 2017;4(11):2788-92.
45. Miller B. Split-Ring Disk Study of Anodic Processes at a Copper Electrode in Alkaline Solution. Journal of the Electrochemical Society. 1969;116(12):1675-&.
46. Juska VB, Pemble ME. A dual-enzyme, micro-band array biosensor based on the electrodeposition of carbon nanotubes embedded in chitosan and nanostructured Au-foams on microfabricated gold band electrodes. Analyst. 2019.